Available online at www.sciencedirect.com
SCIENCE DIRECT®
Bioorganic Chemistry 32 (2004) 178–191
BIOORGANIC CHEMISTRY
www.elsevier.com/locate/bioorg

# Slow-binding inhibition of peptide deformylase by cyclic peptidomimetics as revealed by a new spectrophotometric assay

Kiet T. Nguyen, Xubo Hu, and Dehua Pei*

*Department of Chemistry and Ohio State Biochemistry Program, The Ohio State University, 100 West 18th Avenue, Columbus, OH 43210, USA*

Received 12 November 2003

**Abstract**

A new spectrophotometric/fluorimetric assay for peptide deformylase (PDF) has been developed by coupling the PDF reaction with that of dipeptidyl peptidase I (DPPI) and using *N*-formyl-Met-Lys-AMC as substrate. Removal of the N-terminal formyl group by PDF renders the dipeptide an efficient substrate of DPPI, which subsequently removes the dipeptidyl units to release 7-amino-4-methylcoumarin as the chromophore/fluorophore. The PDF reaction is conveniently monitored on a UV–Vis spectrophotometer or a fluorimeter in a continuous fashion. The utility of the assay was demonstrated by determining the catalytic activity of PDF and the inhibition constants of PDF inhibitors. These studies revealed the slow-binding behavior of a previously reported macrocyclic PDF inhibitor. This method offers several advantages over the existing PDF assays and should be particularly useful for screening PDF inhibitors in the continuous fashion.


*Keywords:* Peptide deformylase; Kinetics; Assay; Dipeptidyl peptidase; PDF inhibition

## 1. Introduction

Protein synthesis in prokaryotes initiates with an *N*-formylmethionyl-tRNA$_i$, resulting in N-terminal formylation of all nascent polypeptides. Peptide deformylase

* Corresponding author. Fax: 1-614-292-1532.
*E-mail address:* pei.3@osu.edu (D. Pei).

0045-2068/$ - see front matter © 2004 Elsevier Inc. All rights reserved.
doi:10.1016/j.bioorg.2004.01.001

(PDF,[1] EC 3.5.1.88) catalyzes the subsequent removal of the formyl group from the majority of bacterial proteins [1]. PDF belongs to a new subclass of amide hydrolase, which utilizes a tetrahedrally coordinated ferrous ion to activate the metal–bound water for nucleophilic attack on the substrate formyl group [2–4]. Genetic studies have shown that PDF is essential for bacterial survival [5–7], but has apparently no catalytic function in mammals [8]. PDF is present in all bacterial organisms whose genomes have been sequenced. These properties make PDF an attractive target for designing novel, broad-spectrum antibacterial agents [9–11]. Many potent PDF inhibitors have been reported in recent years, some of which showed excellent antibacterial activity in vitro and in animal models [12–16]. One of these inhibitors is currently in phase I clinical trials for the treatment of upper respiratory tract infections.

To facilitate the mechanistic study of PDF and inhibitor screening, we and others have developed several assay methods for this enzyme. One method monitors the release of formate, using a formate dehydrogenase (FDH) as the coupling enzyme [17,18]. Due to the poor specific activity of formate dehydrogenases, this assay does not work well in the continuous fashion for assaying potent inhibitors. A second assay employs *N*-formylmethionylleucyl-*p*-nitroanilide (f-ML-*p*NA) as substrate and the deformylation reaction was coupled to *Aeromonas* aminopeptidase (AAP), which hydrolyzes the product, Met-Leu-*p*-nitroanilide, to release the chromogenic *p*-nitroaniline [19]. This convenient, sensitive, and inexpensive assay has been the primary method used in this laboratory for mechanistic studies. However, the coupling enzyme AAP is also a metallopeptidase and is strongly inhibited by most of the PDF inhibitors. Finally, a third assay employs *N*-formyl-(β-thiaphenylalanine)-containing peptide substrates that eliminate thiophenol upon PDF catalyzed hydrolysis of the formyl group [20]. The released thiophenol is monitored spectrophotometrically using Ellman's reagent, 5,5′-dithiobis(2-nitrobenzoic acid) (DTNB). This assay proves to be highly sensitive and convenient for high-throughput screening of non-thiol-containing PDF inhibitors. Its drawback is that the substrate is accessible only by multiple-step synthesis and can undergo spontaneous (albeit slow) release of thiophenol in aqueous solution. Further, we have recently synthesized a macrocyclic PDF inhibitor **1** (Fig. 1), in which the P1′ and P3′ side chains are covalently cross-linked [16]. The macrocycle acts as a potent, slow-binding inhibitor. We experienced major difficulties in its kinetic characterization using the existing assays. These difficulties prompted us to develop yet another spectrophotometric assay of PDF in which the PDF reaction is coupled to dipeptidyl peptidase I (DPPI, also called cathepsin C). DPPI is a cysteine protease of high specific activity toward peptide substrates [21]. Because PDF inhibitors do not generally inhibit DPPI, the assay was conveniently carried out in the continuous fashion and used to fully characterize the slow-binding inhibitor.

[1] *Abbreviations used*: PDF, peptide deformylase; DPPI, dipeptidyl peptidase I; f-Met-Lys-AMC, 7-(*N*-formylmethionyl-L-lysyl)amino-4-methylcoumarin.

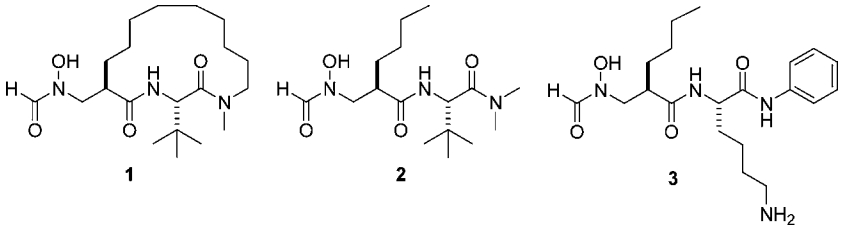


Fig. 1. Structures of PDF inhibitors.

## 2. Materials and methods

### 2.1. Materials

*Escherichia coli* PDF was overexpressed in *E. coli* and purified to apparent homogeneity with either $Fe^{2+}$ or $Co^{2+}$ as the divalent metal [4,18]. DPPI from bovine spleen and yeast formate dehydrogenase were purchased from Sigma Chemical (St. Louis, MO). Other chemicals were obtained from either Sigma–Aldrich (St. Louis, MO) or Bio-Rad Laboratories (Hercules, CA) and Advanced ChemTech (Louisville, KY). PDF inhibitors **1**–**3** were synthesized as previously described [8,16].

### 2.2. Analytical methods

Protein concentration was determined by Bradford assay using bovine serum albumin as the protein standard. For PDF, the total protein concentration as determined by Bradford assay was corrected by a factor of 0.71 [4]. Substrate concentrations were determined by base hydrolysis followed by measuring the absorbance of 7-amino-4-methylcoumarin at 360 nM ($\varepsilon = 1.7 \times 10^4\ M^{-1}\ cm^{-1}$).

### 2.3. 7-($N^{\alpha}$-Benzyloxycarbonyl-$N^{\varepsilon}$-t-butoxycarbonyl-L-lysyl)amino-4-methylcoumarin [N-Cbz-Lys(Boc)-AMC]

To a solution of Cbz-Lys(Boc)-OH (0.42 g, 1.1 mmol), 7-amino-4-methylcoumarin (0.17 g, 1.0 mmol) and HOBt (0.17 g, 1.1 mmol) in dichloromethane (10 mL) was added EDC (0.23 g, 1.2 mmol) at 0 °C. The reaction was stirred overnight at room temperature. The mixture was diluted with 80 mL of ethyl acetate and washed with dilute HCl ($2 \times 20$ mL), water (20 mL), 5% $NaHCO_3$ ($2 \times 20$ mL), and brine (20 mL). The organic layer was dried over $Na_2SO_4$, filtered and concentrated to dryness. The residue was subjected to flash chromatography using dichloromethane/ethyl acetate as eluent to afford 190 mg of a white solid (35% yield). $^1H$ NMR ($CDCl_3$, 250 MHz) $\delta$ 9.22 (s, 1H), 7.54 (s, 1H), 7.25 (m, 6H), 6.00 (s, 1H), 5.84 (d, $J = 7.5$ Hz, 1H), 4.99 (s, 2H), 4.65 (br s, 1H), 4.27 (m, 1H), 2.97 (m, 2H), 2.23 (s, 3H), 1.82 (m, 1H), 1.35 (m, 4H), 1.28 (s, 9H).

### 2.4. 7-(*N*-formylmethionyl-$N^{\varepsilon}$-t-butoxycaronyl-L-lysyl)amino-4-methylcoumarin [f-Met-Lys(Boc)-AMC]

*N*-Cbz-Lys(Boc)-AMC (90 mg, 0.17 mmol) was dissolved in a mixture solvent containing 1:1 (v/v) methanol and ethyl acetate (10 mL) and hydrogenated in the presence of Pd/C at room temperature for 2.5 h. After the reaction was completed the catalyst was removed by filtration and the filtrate was concentrated to dryness. The residue was dissolved in dichloromethane (6 mL), *N*-formylmethionine (37 mg, 0.21 mmol), HOBt (32 mg, 0.21 mmol), and EDC (40 mg, 0.21 mmol) were sequentially added at 0 °C. The mixture was stirred for 2 h at room temperature. After that the mixture was diluted with 50 mL of ethyl acetate, washed with dilute HCl ($2 \times 15$ mL), water (15 mL), 5% $NaHCO_3$ ($2 \times 15$ mL), and brine (15 mL). The organic layer was dried over $Na_2SO_4$, filtered and concentrated to dryness. The residue was purified by silica column chromatography using dichloromethane/ethyl acetate as eluent to give 60 mg of product (64% yield for two steps). $^1$H NMR ($CDCl_3$, 250 MHz) $\delta$ 9.76, (s, 1H), 8.28 (s, 1H), 7.84 (d, $J = 7.5$ Hz, 1H), 7.68 (d, $J = 7.5$ Hz, 1H), 7.65 (s, 1H), 7.42 (m, 2H), 6.12 (s, 1H), 4.91 (m, 2H), 4.67 (m, 1H), 3.07 (m, 2H), 2.63 (m, 2H), 2.36 (s, 3H), 2.20–2.03 (m, 2H), 2.05 (s, 3H), 1.95 (m, 1H), 1.83 (m, 1H), 1.45 (m, 4H), 1.39 (s, 9H).

### 2.5. 7-(*N*-Formylmethionyl-L-lysyl)amino-4-methylcoumarin (f-Met-Lys-AMC)

f-Met-Lys(Boc)-AMC (50 mg) was dissolved in dichloromethane (2 mL) and trifluoroacetic acid (1 mL) was added. After the mixture was stirred for 2 h, the volatile substances were removed under vacuum to afford the product in quantitative yield. The product was neutralized by dissolving in 1:1 (v/v) dichloromethane/isopropyl alcohol (10 mL) containing 10% triethylamine. $^1$H NMR ($D^6$-DMSO, 250 MHz): $\delta$ 10.45 (s, 1H), 8.37 (m, 2H), 8.04 (br s, 1H), 7.76 (m, 2H), 7.65 (br s, 3H), 7.50 (dd, $J = 2.0$, 8.7 Hz), 6.27 (s, 1H), 4.44 (m, 2H), 2.79 (m, 2H), 2.46 (m, 2H), 2.40 (s, 3H), 2.04 (s, 3H), 1.85–1.49 (m, 8H). ESI-HRMS: calcd for $C_{22}H_{31}N_4O_5S^+$ ($M + H^+$): 463.2009. Found 463.2004.

### 2.6. 7-($N^{\alpha}$-9-fluorenylmethoxycarbonyl-$N^{\gamma}$-trityl-L-glutamyl)amino-4-methylcoumarin [N-Fmoc-Gln(Trt)-AMC]

To an ice-chilled solution of Fmoc-Gln(Trt)-OH (244 mg, 0.4 mmol) and triethylamine (40 mg, 0.4 mmol) in tetrahydrofuran (7 mL), ethyl chloroformate (48 mg, 0.44 mmol) was added dropwise. The mixture was stirred at 0 °C for 10 min. 7-Amino-4-methylcoumarin (68 mg, 0.4 mmol) was added and the solution was stirred overnight at room temperature. The solvent was evaporated and the residue was dissolved in 50 mL of dichloromethane and washed with 0.5 M HCl ($2 \times 20$ mL), water (20 mL), 5% $NaHCO_3$ ($2 \times 20$ mL), and brine (20 mL). The organic layer was dried over $Mg_2SO_4$, filtered, and concentrated. The crude product was purified by silica gel chromatography using dichloromethane/ethyl acetate as eluent to give 40 mg of a white solid. $^1$H NMR ($CDCl_3$, 400 MHz): $\delta$ 7.77 (d, $J = 5$ Hz, 1H), 7.49 (s, 1H),

7.44 (s, 1H), 7.40–7.27 (m, 26H), 6.97 (s, 1H), 6.18 (s, 1H), 4.41 (br s, 1H), 4.15 (m, 2H), 2.80 (m, 2H), 2.55 (m, 2H), 2.39 (s, 3H).

### 2.7. 7-(*N*-Formylmethionyl-L-glutamyl)amino-4-methylcoumarin (f-Met-Gln-AMC)

*N*-Fmoc-Glutamyl(Trt)-AMC (40 mg, 0.053 mmol) was dissolved in 20% piperidine dichloromethane (5 mL) and stirred at room temperature for 45 min. The reaction was purified by silica gel chromatography using ethyl acetate/dichloromethane as eluent to give 20 mg white solid. The residue was redissolved in dichloromethane (7 mL), and *N*-formylmethionine (8.8 mg, 0.05 mmol), 1-hydroxy-7-azabenzotriazole (0.037 mmol), and 1-ethyl-3-(-(dimethylamino)propyl)-carbodiimide (EDC) (7.6 mg, 0.038 mmol) were sequentially added at 0 °C. The reaction was stirred overnight at room temperature and followed by dilution into 40 mL dichloromethane. The mixture was washed with 0.5 M HCl ($2 \times 20$ mL), water (20 mL), 5% $NaHCO_3$ ($2 \times 20$ mL) and brine (20 mL). The organic layer was dried over $Mg_2SO_4$, filtered, and concentrated. The residue was purified by silica gel column chromatography using dichloromethane/ethyl acetate as eluent to give 15 mg of 7-($N^{\alpha}$-formylmethionyl-*N*-trityl-L-glutamyl)amino-4-methylcoumarin (58% yield). This purified compound (15 mg) was dissolved in 4.5 mL trifluoroacetic acid, 0.25 mL thioanisole, 0.1 mL anisole, and 0.15 mL ethanedithiol. The mixture was stirred at room temperature for 1 h and followed with removing the volatile substances with nitrogen gas. The remaining residue was triturated with ether ($3 \times 15$ mL) to give 10 mg of white solid (quantitative yield). The product was neutralized by redissolving in 1:1 dichloromethane/isopropyl alcohol containing 10% triethylamine (10 mL). The solvent was evaporated by nitrogen gas and the residue was triturated with ether ($2 \times 15$ mL). $^1$H NMR (DMSO, 400 MHz) $\delta$ 10.42 (s, 1H), 8.41 (d, $J = 4$ Hz, 1H), 8.34 (d, $J = 4$ Hz, 1H), 8.10 (s, 1H), 7.77 (m, 2H), 7.52 (d, $J = 4$ Hz, 1H), 7.3 (s, 1H), 6.80 (s, 1H), 6.28 (s, 1H), 4.46 (m, 1H), 4.37 (m, 1H), 2.5 (m, 2), 2.4–2.2 (m, 6H), 2.15 (s, 1H), 2.05 (s, 3H), 1.92 (s, 3H). ESI-HRMS: calcd for $C_{21}H_{26}N_4O_6SNa^+$ ($M + Na^+$): 485.1465. Found: 485.1465.

### 2.8. Continuous PDF assay with DPPI

Prior to use, DPPI was activated by the treating with 5 mM dithiothreitol (DTT) for 30 min in 50 mM Hepes (pH 7.0), 10 mM NaCl. Unless stated otherwise, all assays were performed at room temperature (25 °C). Assay reactions were performed in a quartz microcuvette (total reaction volume = 200 μL) containing 5–150 μM substrate, 50 mM Hepes (pH 7.0), 10 mM NaCl, 5 mM DTT, and 0.1 U of DPPI. Assay reactions were initiated by the addition of 1–10 μL of Co(II)-PDF enzyme (final concentration of 0.5–2.5 nM) and monitored continuously at 360 nm with a Perkin–Elmer Lambda 20 UV–Vis spectrophotometer. The initial rates were obtained from the early part of the reaction progression curves (<60 s). To insure that the deformylation reaction is the rate-limiting, reactions at the lowest and highest substrate concentrations were repeated with doubled amount of DPPI (0.2 U). The amount of background hydrolysis of f-Met-Lys-AMC or f-Met-Gln-AMC by DPPI was

determined under similar conditions but in the absence of PDF. This background hydrolysis rate was subtracted from the observed reaction rates.

To determine the catalytic activity of DPPI toward Met-Lys-AMC, a stock solution of f-Met-Lys-AMC (10 mM) in 50 mM Hepes (pH 7.0), 150 mM NaCl was incubated overnight with excess Co(II)-PDF to allow complete hydrolysis of the *N*-formyl moiety. The PDF was inactivated by heating at 95 °C for 30 min and removed by centrifugation. DPPI assays were performed by adding 0.005 U of DPPI to a mixture (200 μL) containing 50 mM Hepes (pH 7.0), 10 mM NaCl, 5 mM DTT, and 0.5–100 μM of Met-Lys-AMC. The reaction progress was monitored at 360 nm. The catalytic activity of DPPI against Met-Gln-AMC was determined in a similar manner.

### 2.9. PDF inhibition assay

PDF inhibition assays were performed in a reaction mixture (200 μL) containing 100 μM f-Met-Lys-AMC, 0–200 nM inhibitor, 50 mM Hepes (pH 7.0), 10 mM NaCl, 5 mM DTT, and 0.1 U of DPPI. The background hydrolysis rate was measured by monitoring the reaction for 30 s at 360 nm on a spectrophotometer. The PDF reaction was then initiated by the addition of Co(II)-PDF (final concentration 4.0 nM) and monitored continuously for another 60–120 s. Initial rate was calculated from the early region of the reaction progress curve (0–30 s after addition of PDF) and corrected by subtracting the background rate. The inhibition constant ($K_I$) was calculated according to the equation:

$$V = (V_{max} \times [S])/(K_M(1 + [I]/K_I) + [S]).$$

PDF assay in the fluorescence mode was similarly performed except that the reaction was monitored on an Aminco-Bowman Series 2 Luminescence spectrometer. The excitation and emission wavelengths were set at 380 and 460 nm, respectively.

Activity and inhibition assays with Fe(II)-PDF were carried out in the same manner as for Co(II)-PDF, except that the reaction buffer contained 1 mM tris(carboxyethyl)phosphine instead of 5 mM DTT as the reducing agent [3].

### 2.10. Slow-binding inhibition of PDF

To determine the $K_I$ value, assay reaction (200 μL) contained 60 μM f-Met-Lys-AMC, 0.15 U DPPI, 50 mM Hepes (pH 7.0), 30 mM NaCl, 5 mM DTT, and 0–500 nM inhibitor **1**. The reaction was initiated by the addition of Co(II)-PDF (2.0 nM final concentration) and was monitored continuously at 360 nm on a UV–Vis spectrophotometer. The initial reaction rate was obtained from the early region of the reaction progress curve (0–60 s), during which the substrate to product conversion was <20%. The obtained initial rates (which were corrected for background hydrolysis) were fitted to the Michaelis–Menten equation to produce the $K_I$ value. To determine the $K_I^*$ value, the assay reaction (1000 μL) containing 50 mM Hepes (pH 7.0), 100 mM NaCl, 4.0 nM PDF, 0–40 nM inhibitor **1**, and 100 μg/mL bovine serum albumin was incubated on ice for 4 h. The mixture was then brought to room temperature and adjusted to 3 mM DTT, and the reaction was initiated by the addition

of 0.5 U of DPPI and 70 μL of f-Met-Lys-AMC (final 200 μM). The initial reaction rates were similarly obtained and fitted to the Michaelis–Menten equation to produce the $K_I^*$ value. Reactivation of the E · I* complex was carried out by incubating a reaction solution (100 μL) containing 50 mM Hepes (pH 7.0), 150 mM NaCl, PDF (40–160 nM), inhibitor **1** (50–200 nM), and 100 μg/mL BSA for 2 h on ice. The solution was rapidly diluted into 900 μL of a solution containing 50 mM Hepes (pH 7.0), 150 mM NaCl, 5 mM DTT, 270 μM f-Met-Lys-AMC, and 0.1 U of DPPI and the reaction progress was monitored continuously at 360 nm.

## 3. Results and discussion

### 3.1. Assay design

An ideal assay should involve a highly efficient substrate for both PDF and the coupling enzyme, and the PDF inhibitors should not significantly inhibit the coupling enzyme. DPPI meets both of these requirements. First, since DPPI is a cysteine protease and has an entirely different catalytic mechanism from PDF [21], we reasoned that the metal-chelating PDF inhibitors should not inhibit DPPI. Second, DPPI efficiently hydrolyzes a wide variety of dipeptidyl AMC substrates to release the corresponding dipeptides and the chromophore/fluorophore AMC [22]. Substrate specificity studies of PDF have revealed a strong preference for an L-methionine at the N-terminal position [23–25]. It has broad specificity at the penultimate position, although amino acids with positively charged side chains are slightly preferred [25]. On the basis of the above considerations, we designed a dipeptide substrate, f-Met-Lys-AMC (Fig. 2), for the new DPPI coupled assay. The presence of a polar side chain at the penultimate position also improves the aqueous solubility of the substrate. Sequential action by PDF and DPPI should release formate, dipeptide Met-Lys, and the AMC, which can be monitored by either its absorbance at 360 nm or fluorescence emission at 460 nm. Consistent with a previous report [22], the hydrolysis of Met-Lys-AMC by DPPI is extremely fast, with a $k_{cat}$ value of 5.7 $s^{-1}$, $K_M$ of 2.8 μM, and a $k_{cat}/K_M$ of $2.1 \times 10^6$ $M^{-1}$ $s^{-1}$ at pH 7.0. The low $K_M$ value makes DPPI a particularly suitable coupling enzyme.

### 3.2. Continuous DPPI coupled assay

Fig. 3A shows the time courses for the hydrolysis of f-Met-Lys-AMC (50 μM) by various amounts of Co(II)-PDF and DPPI, monitored at 360 nm on a UV–Vis spectrophotometer. In the presence of 0.03 U of DPPI and 5.0 nM of PDF, the substrate is rapidly hydrolyzed and the absorbance increased linearly with time (tracing A). The initial rate for f-Met-Lys-AMC hydrolysis approximately doubles when the amount of PDF is doubled (compare tracings A and B). However, when the amount of DPPI is doubled while keeping the amount of PDF constant, there is no significant increase in hydrolysis rate (compare tracings A and C). Further, there is no visible lag phase at the early regions of the curves. These results indicate that under the

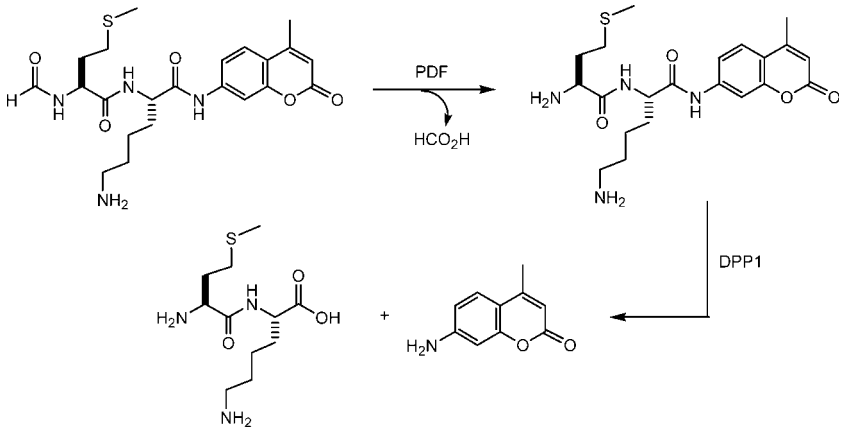


Fig. 2. Reactions involved in the assay.

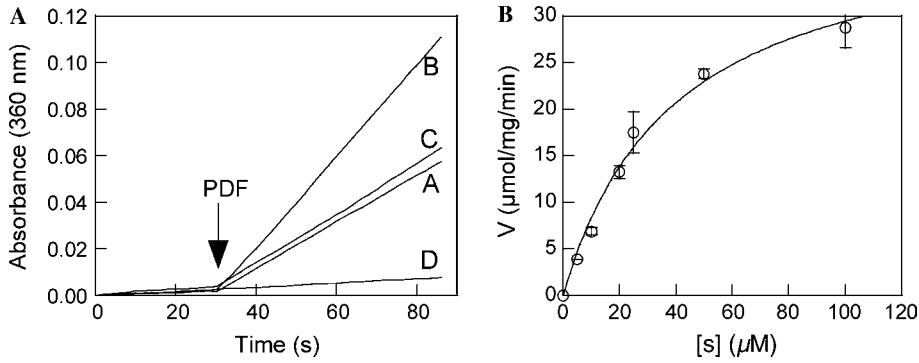


Fig. 3. (A) Time courses for the hydrolysis of f-Met-Lys-AMC by PDF. In a final volume of 200 μL (pH 7.0), f-Met-Lys-AMC (80 μM) was incubated with varying amounts of Co(II)-PDF and DPPI. Tracing A, 2 nM PDF and 0.03 U DPPI; tracing B, 4 nM PDF and 0.03 U DPPI; tracing C, 2 nM PDF and 0.06 U DPPI; and tracing D, 0.03 U DPPI (no PDF). (B) Plot of initial rates against f-Met-Lys-AMC concentration. The curve was fitted to the data according to the equation, $V = k_{cat} \times [E] \times [S]/(K_M + [S])$, to give a $k_{cat}$ of $26 \pm 4\ s^{-1}$ and $K_M$ of $40 \pm 7$ μM. (Data presented are the mean ± SD for three independent experiments.)

assay conditions, the PDF reaction is rate limiting. In the absence of PDF, we also observed a small yet clearly detectable background hydrolysis of the substrate (tracing D). To determine the origin of this activity, we treated DPPI with p-hydroxy-α-bromoacetophenone [26], which selectively inhibits cysteine proteases [27] by alkylating their active-site cysteines, prior to assay with Met-Lys-AMC and f-Met-Lys-AMC. Similar reduction of activity toward both substrates was observed. This suggests that the background signal was due to direct hydrolysis of f-Met-Lys-AMC by DPPI (with f-Met-Lys and AMC as reaction products). Further kinetic analysis (in the absence of PDF) revealed a $k_{cat}$ value of $0.06\ s^{-1}$, $K_M$ value of 82 μM, and a

$k_{cat}/K_M$ value of 760 $M^{-1} s^{-1}$ for DPPI hydrolysis of f-Met-Lys-AMC. In an attempt to minimize the amount of background hydrolysis, we chemically synthesized another substrate, f-Met-Gln-AMC, but found that the commercial DPPI preparation also cleaved this substrate with similar catalytic efficiency, providing further evidence that DPPI is responsible for the background signal. Fortunately, this background reaction can be easily measured and corrected, and therefore does not complicate the assay in any substantial manner. To correct for this background rate, we typically monitored the reaction for 30 s prior to the addition of PDF (Fig. 3A); the slope of the line gives the background hydrolysis rate. After the addition of PDF, the reaction is monitored for another 60 s to obtain the total hydrolysis rate. Subtraction of the background rate from the latter gives the PDF reaction rate. The total amount of substrate consumed during the entire 90 s assay period is well below <20%. The slightly increased slope of tracing C relative to A reflects the increased amount of background hydrolysis of f-Met-Lys-AMC as a result of doubling the amount of DPPI.

f-Met-Lys-AMC is an excellent substrate of PDF and exhibits Michaelis–Menten kinetics (Fig. 3B). For Co(II)-PDF, the catalytic constants are $k_{cat}$ of $26 \pm 4\ s^{-1}$, $K_M$ of $40 \pm 7\ \mu M$, and $k_{cat}/K_M$ of $(6.5 \pm 1.1) \times 10^5\ M^{-1} s^{-1}$ at pH 7.0. A $k_{cat}/K_M$ value of $7.5 \times 10^5\ M^{-1} s^{-1}$ was obtained for the same substrate by the formate dehydrogenase assay in the end-point format. The catalytic constants toward Fe(II)-PDF under the same conditions were similarly determined as $52 \pm 1\ s^{-1}$, $39 \pm 2\ \mu M$, and $(1.3 \pm 0.1) \times 10^6\ M^{-1} s^{-1}$, respectively. These activities are only slightly lower than that of f-ML-*p*NA, the best PDF substrate previously reported ($k_{cat}/K_M = 1.9 \times 10^6\ M^{-1} s^{-1}$) [19]. Coupled with the large extinction coefficient of AMC ($\varepsilon = 17,000\ M^{-1} cm^{-1}$), the current method is highly sensitive. Actually, the sensitivity of this assay is further improved by monitoring the reaction in the fluorescence mode. This is critical for assaying very potent PDF inhibitors, because a proper assay condition requires that the enzyme concentration be lower than that of the inhibitor, which should in turn be similar to the $K_I$ value.

### 3.3. Screening of PDF inhibitors

The utility of the new assay in PDF inhibitor screening was first demonstrated with BB-3497 (Fig. 1, compound **2**), a competitive inhibitor of PDF ($IC_{50}$ ~7 nM against Ni(II)-EcPDF) [15]. Varying concentrations of BB-3497 were directly added into the assay reaction and the reaction progress was monitored continuously at 360 nm on a spectrophotometer or at 460 nm on a spectrofluorimeter (excitation at 380 nm). Fig. 4 shows an example of the reaction progress curves obtained with Co(II)-PDF, as monitored on a spectrofluorimeter. The fluorescence yield increased linearly with time and the initial rates were calculated from the slopes of the lines. Data fitting to the Michaelis–Menten equation gave a $K_I$ value of $23 \pm 5$ nM against Co(II)-PDF. A $K_I$ value of $9.3 \pm 1.9$ nM was similarly determined for Fe(II)-PDF. These values are in reasonable agreement with the reported $IC_{50}$ value (~7 nM) [15]. Using the same assay method, compound **3** (Fig. 1) gave a $K_I$ value of $17 \pm 2$ nM against Co(II)-PDF. Assays in the absorption mode gave very similar $K_I$ values for

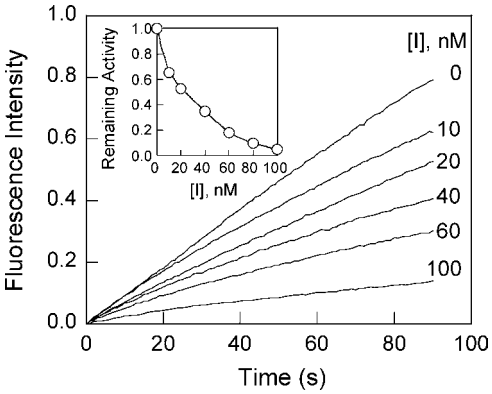


Fig. 4. Inhibition of PDF by BB-3497. Reactions were carried out at pH 7.0 using f-Met-Lys-AMC as substrate (40 μM) and in the presence of indicated amounts of inhibitor. The reaction was initiated by the addition of 4 nM Co(II)-PDF as the final component and the fluorescence yield at 460 nm (excitation at 380 nm) was monitored with time (no correction of background rate). Inset, plot of remaining activity (after correction for background hydrolysis and relative to that in the absence of inhibitor) against inhibitor concentration. Data fitting against the equation, $V = (V_{max} \times [S])/(K_M(1 + [I]/K_I) + [S])$, gave a $K_I$ value of $23 \pm 5$ nM.

these two inhibitors. Previous AAP assays with Co(II)-PDF (in the end-point format) gave $K_I$ values of $11 \pm 1$ and $18 \pm 1$ nM for compounds **2** and **3**, respectively [8]. We have also used this new assay method to successfully determine the $K_I$ values for a variety of inhibitors against *E. coli*, *Plasmodium falciparum*, and human PDF (to be reported elsewhere). Under the assay conditions, none of the PDF inhibitors showed any inhibition of DPPI (assayed with Met-Lys-AMC as substrate).

### *3.4. Slow-binding inhibition of macrocycle **1***

Compound **1** exhibited time-dependent inhibition of EcPDF; drastically different $IC_{50}$ values were obtained depending on the duration of preincubation of the enzyme with the inhibitor. In our earlier work [16], only an apparent $K_I$ value (0.23–0.67 nM) was obtained after preincubating PDF with compound **1** for 2 h. Time-dependent enzyme inhibition is usually caused by either time-dependent inactivation (e.g., covalent modification) of the enzyme or slow-binding inhibition (slow conversion of an initial $E \cdot I$ complex to a tighter $E \cdot I^*$ complex). Since inhibition by **1** is reversible (vide infra), slow-binding inhibition must be operative and can be described by equation

$$E + I \overset{K_I}{\rightleftarrows} E \cdot I \underset{k_6}{\overset{k_5}{\rightleftarrows}} E \cdot I^*,$$

where $K_I$ is the equilibrium constant for the formation of the initial $E \cdot I$ complex, whereas $k_5$ and $k_6$ are the forward and reverse rate constants for the slow interconversion of $E \cdot I$ and $E \cdot I^*$, respectively. The overall potency of the inhibitor is described by the equilibrium constant $K_I^* = K_I \cdot k_6/(k_5 + k_6)$ [28]. However, proper kinetic characterization of this inhibitor proved very challenging using the existing

assays. Fig. 5A shows an example of PDF reaction progress curves in the absence (tracings A and B) and the presence of compound **1** (50 nM, tracing C), using FDH as the coupling enzyme [17,18]. Instead of decreasing PDF reaction rate with time (as expected from the time-dependent conversion of $E \cdot I$ into $E \cdot I^*$), an apparent time-dependent "activation" was observed. This lag phase is due to slow FDH reaction during the early stage; as formate accumulates, the FDH reaction rates increases, eventually reaching the steady state when the rate of FDH reaction equals that of PDF reaction. The observed lag phase became even more pronounced when compound **1** was added to the assay reaction (tracing C). Addition of large amounts of FDH did not significantly improve the situation [compare tracings A (reaction contained 2.5 U/mL FDH) and B (reaction contained 12.5 U/mL FDH)].

Fig. 5B shows the reaction progress curves of the same experiments, but with DPPI as the coupling enzyme. The addition of compound **1** to the assay reaction resulted in time-dependent inhibition. Importantly, none of the reaction progress curves had any visible lag phase. Further, when assayed against Met-Lys-AMC, compound **1–3** did not show any detectable inhibition of DPPI at concentrations up to 500 nM (data not shown). Data fitting against Michaelis–Menten equation using the initial reaction rates (0–60 s) and the final steady-state rates (after preincubation for 4 h) produced $K_I$ and $K_I^*$ values of $96 \pm 16$ and $0.31 \pm 0.14$ nM, respectively, for inhibitor **1**. The latter is in excellent agreement with the apparent $K_I$ value previously determined using the FDH and AAP assays (0.23–0.67 nM) [16]. To determine the reverse rate constant $k_6$, PDF and compound **1** was preincubated for 2 h and then rapidly diluted into 900 μL of a reaction buffer containing f-MK-AMC. The time-dependent recovery of PDF activity was monitored with time on a spectrophotometer (Fig. 6). Data fitting the data against the equation

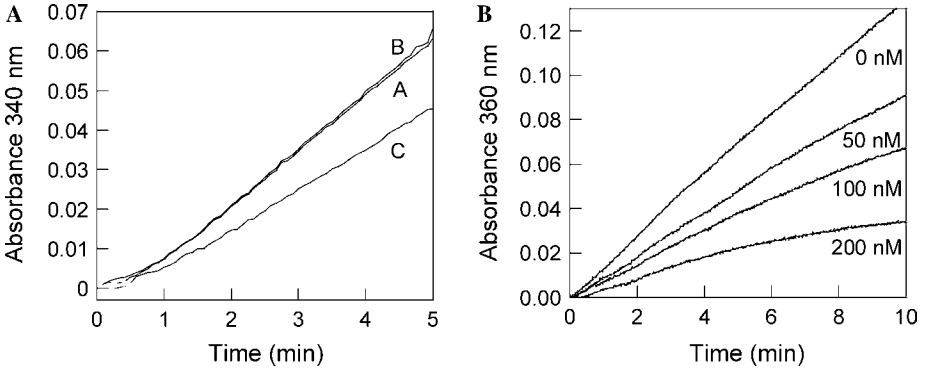


Fig. 5. (A) Time courses for FDH-coupled reactions. Each reaction (200 μL total volume) contained 50 mM $K_2HPO_4$ (pH 7.2), 6.0 nM Co(II)-PDF, and 225 μM f-Met-Lys-AMC. In addition, reactions A and B contained 0.5 and 2.5 U of FDH, respectively, whereas reaction C contained 0.5 U FDH and 50 nM compound **1**. (B) Time courses for DPPI-coupled reactions. Each reaction (200 μL total volume) contained 50 mM Hepes (pH 7.0), 30 mM NaCl, 5 mM DTT, 3.0 nM PDF, 0.022 U of DPPI, 225 μM f-Met-Lys-AMC, and indicated amounts of compound **1**.

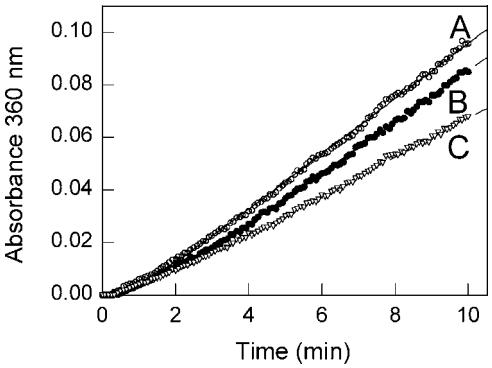


Fig. 6. Reactivation of inhibited PDF. Co(II)-PDF (80–100 nM) and compound **1** (50–150 nM) were incubated on ice for 2 h. The resulting enzyme (100 μL) was rapidly diluted into a reaction solution (900 μL) containing 270 μM f-Met-Lys-AMC and 0.1 U of DPPI. (A) 80 nM PDF and 50 compound **1**; (B) 80 nM PDF and 100 nM compound **1**; (C) 120 nM PDF and 150 nM compound **1**. Curves were fitted to the data according to the equation, $\mathrm{Abs}_{360} = v_s[t - (1 - e^{k_6 t})/k_6]$, to give a rate constant ($k_6$) of $0.0037 \pm 0.0010\,\mathrm{min}^{-1}$.

$$\mathrm{Abs}_{360\,\mathrm{nm}} = v_s[t - (1 - e^{k_6 t})/k_6].$$

gave the reverse rate constant $k_6$ ($0.0037 \pm 0.0010\,\mathrm{min}^{-1}$). The forward rate constant, $k_5$, was calculated from the $K_I$, $K_I^*$, and $k_6$ values to be $1.6 \pm 0.4\,\mathrm{min}^{-1}$.

## 4. Conclusion

In summary, we have developed yet another highly sensitive, convenient, and rapid assay for peptide deformylase. Compared to the previously reported assays, a major advantage of the current method is that the assay reaction can be carried out in a continuous fashion in the presence of PDF inhibitors, making it particularly useful for screening PDF inhibitors in a high-throughput setting and the kinetic characterization of PDF inhibitors. This feature has allowed us to characterize the slow-binding properties of macrocyclic PDF inhibitor **1**, which had been difficult to accomplish by the other methods. It should be noted that, because PDF inhibitors usually do not inhibit the formate dehydrogenase either, the FDH assay [17,18] has been widely used for PDF inhibitor screening. However, due to the poor specific activity of FDH, the FDH assays were typically performed in an end-point fashion. As such, the FDH assay is not suitable (at least not convenient) for the kinetic evaluation of slow-binding inhibitors. Its lower sensitivity and end-point nature also make the FDH assay less reliable for determining the $K_I$ values of exceptionally potent PDF inhibitors. A drawback of the current assay is the presence of slight background hydrolysis of *N*-formylated substrates by DPPI. This is not a problem for routine kinetic assays or inhibitor screening involving the wild-type PDF. However, this background reaction may become significant and thus complicate the assay results involving catalytically impaired PDF mutants.

Considering the strengths and weaknesses of each of the PDF assays, we make the following recommendations. For routine kinetic assays of wild-type and mutant PDF in the absence of PDF inhibitors, the AAP assay [19] is most convenient. Both FDH and DPPI assays may be employed to screen PDF inhibitors. If kinetic characterization of a PDF inhibitor is desired or if the PDF inhibitor is exceptionally potent (low $K_I$ value), the DPPI assay is the method of choice. Further, for applications that require high substrate concentrations, we prefer the DPPI assay in the absorbance mode, as high concentration can lead to internal fluorescence quenching and other complications. However, for determining the $K_I$ values of potent PDF inhibitors, the fluorescence mode is advantageous, as it is more sensitive allowing the use of very low enzyme (e.g., 2 nM) and substrate concentrations.

## Acknowledgment

This work was supported by a grant from the National Institutes of Health (AI40575).

## References

[1] T. Meinnel, Y. Mechulam, S. Blanquet, Biochimie 75 (1993) 1061–1075.
[2] P.T.R. Rajagopalan, X.C. Yu, D. Pei, J. Am. Chem. Soc. 119 (1997) 12418–12419.
[3] D. Groche, A. Becker, I. Schlichting, W. Kabasch, S. Schultz, A.F.V. Wagner, Biochem. Biophys. Res. Commun. 246 (1998) 342–346.
[4] P.T.R. Rajagopalan, S. Grimme, D. Pei, Biochemistry 39 (2000) 779–790.
[5] D. Mazel, S. Pochet, P. Marliere, EMBO J. 13 (1994) 914–923.
[6] T. Meinnel, S. Blanquet, J. Bacteriol. 176 (1994) 7387–7390.
[7] P.S. Margolis, C.J. Hackbarth, D.C. Young, W. Wang, D. Chen, Z. Yuan, R. White, J. Trias, Antimicrob. Agents Chemother. 44 (2001) 1825–1831.
[8] K.T. Nguyen, X. Hu, C. Colton, R. Chakratarti, M.X. Zhu, D. Pei, Biochemistry 42 (2003) 9952–9958.
[9] D. Pei, Emerg. Ther. Targets 5 (2001) 1–18.
[10] C. Giglione, M. Pierre, T. Meinnel, Peptide deformylase as a target for new generation, broad spectrum antimicrobial agents, Mol. Microbiol. 36 (2000) 1197–1205.
[11] Z. Yuan, J. Trias, R.J. White, Deformylase as a novel antibacterial target, Drug Discov. Today 6 (2001) 954–961.
[12] K.M. Huntington, T. Yi, Y. Wei, D. Pei, Biochemistry 39 (2000) 4543–4551.
[13] D.Z. Chen, D.V. Patel, C.J. Hackbarth, W. Wang, G. Dreyer, D. Young, P.S. Margolis, C. Wu, Z.-J. Ni, J. Trias, R. White, Z. Yuan, Biochemistry 39 (2000) 1256–1262.
[14] C. Apfel, D.W. Banner, D. Bur, M. Dietz, T. Hirata, C. Hubschwerlen, H. Locher, M.G.P. Page, W. Pirson, G. Rosse, J.-L. Specklin, J. Med. Chem. 43 (2000) 2324–2331.
[15] J.M. Clements, R.P. Beckett, A. Brown, G. Catlin, M. Lobell, S. Palan, W. Thomas, M. Whittaker, S. Wood, S. Salama, P.J. Baker, H.F. Rodgers, V. Barynin, D.W. Rice, M.G. Hunter, Antimicrob. Agents Chemother. 45 (2001) 563–570.
[16] X. Hu, K.T. Nguyen, C.L.M.J. Verlinde, W.G.J. Hol, D. Pei, Structure-based design of a macrocyclic inhibitor for peptide deformylase, J. Med. Chem. 46 (2003) 3771–3774.
[17] C. Lazennec, T. Meinnel, Anal. Biochem. 244 (1997) 180–182.
[18] P.T.R. Rajagopalan, A. Datta, D. Pei, Biochemistry 36 (1997) 13910–13918.
[19] Y. Wei, D. Pei, Anal. Biochem. 250 (1997) 29–35.

[20] X.-C. Guo, P.T.R. Rajagopalan, D. Pei, Anal. Biochem. 273 (1999) 298–304.
[21] K. Ishidoh, D. Muno, N. Sato, E. Kominami, J. Biol. Chem. 266 (1991) 16312–16317.
[22] T.V. Tran, K.A. Ellis, C.-M. Kam, D. Hudig, J.C. Powers, Arch. Biochem. Biophys. 403 (2002) 160–170.
[23] J.M. Adams, J. Mol. Biol. 33 (1968) 571–589.
[24] Y.J. Hu, Y. Wei, Y. Zhou, P.T.R. Rajagopalan, D. Pei, Biochemistry 38 (1999) 643–650.
[25] S. Ragusa, P. Mouchet, C. Lazennec, V. Dive, M. Meinnel, J. Mol. Biol. 289 (1999) 1445–1457.
[26] G. Arabaci, X.-C. Guo, K.D. Beebe, K.M. Coggeshall, D. Pei, J. Am. Chem. Soc. 121 (1999) 5085–5086.
[27] E.T. Kaiser, R.W. Furlanetto, J. Am. Chem. Soc. 92 (1970) 6980–6982.
[28] J.F. Morrison, C.T. Walsh, Adv. Enzymol. 61 (1988) 201–301.